

Defect levels of dangling bonds in silicon and germanium through hybrid functionals

Peter Broqvist, Audrius Alkauskas, and Alfredo Pasquarello

*Ecole Polytechnique Fédérale de Lausanne (EPFL), Institute of Theoretical Physics, CH-1015 Lausanne, Switzerland
and Institut Romand de Recherche Numérique en Physique des Matériaux (IRRMA), CH-1015 Lausanne, Switzerland*

(Received 9 June 2008; revised manuscript received 25 July 2008; published 18 August 2008)

Defect levels of dangling bonds in silicon and germanium are determined within their respective band gaps through the use of hybrid density functionals. To validate our approach, we first considered the dangling bond in silicon finding two well-separated defect levels in excellent correspondence with their experimental location. Application to the dangling bond in germanium then yields two very close defect levels lying just above the valence band, which is consistent with the experimental location of the charge neutrality level. The occurrence of negative- U behavior leads to a reduced fraction of neutral dangling bonds, thereby suppressing the electron-spin-resonance activity.

DOI: 10.1103/PhysRevB.78.075203

PACS number(s): 71.55.-i, 71.15.Nc

I. INTRODUCTION

As the scaling of Si-based metal-oxide-semiconductor devices is approaching its technological and physical limits, several materials are being investigated as alternative future solutions. In particular, germanium is currently subjected to a renewed interest owing to its high electron and hole mobilities.^{1,2} Germanium also offers other advantages compared to silicon. Its lower electronic band gap allows for reduced operating voltages^{1,2} and its lower processing temperatures make it more suitable for integration with high- κ dielectric materials.³ However, current state-of-the-art germanium/insulator interfaces show defect densities which exceed operational requirements. While the nature of these defects remains to be identified, the role of the dangling-bond defect is being questioned.⁴ The measured defect density of states at germanium-oxide interfaces lacks the double-peak structure⁴ (characteristic of the silicon dangling bond at the analogous silicon-oxide interfaces).^{5,6} Furthermore, electron-spin-resonance (ESR) experiments at germanium-oxide interfaces do not detect any signal which could be assigned to the germanium dangling bond.⁴ A recent theoretical study relates this behavior to the defect levels of the dangling bond being located below the valence-band edge.⁷ However, in covalent semiconductors, these defect levels are closely related to the charge neutrality level,⁸ which has experimentally been determined in the band gap at ~ 0.1 eV from the valence band.^{9,10}

The theoretical modeling of defect energy levels is not a trivial issue even in the presence of well-identified defect structures. Indeed, the most common electronic-structure methods based on semilocal density-functional calculations severely underestimate electronic band gaps, thereby hindering a direct comparison between theory and experiment. This problem is emphasized in the case of germanium, for which such theoretical schemes give a vanishing band gap. To overcome these difficulties, it appears therefore necessary to resort to electronic-structure methods of higher level.

In this paper, we determine energy levels of dangling-bond defects in silicon and germanium using hybrid density functionals, which incorporate a fraction α of Hartree-Fock exchange. We study the evolution of the defect levels as the

bulk band gap increases with the fraction α . For silicon, the shifts of the band edges are consistent with many-body perturbation theory in the GW approximation¹¹ and the defect levels determined in correspondence of the experimental band gap show excellent agreement with measured values. Application to the dangling-bond defect in germanium results in two close charge-transition levels lying just above the valence band. Their location is consistent with experimental determinations of the charge neutrality level^{9,10} and their small separation accounts for the suppression of the ESR activity.⁴

This paper is organized as follows. The methodological approach is described in Sec. II. In particular, we analyze convergence issues related to the \mathbf{k} -point sampling and the description of charged defects in periodically repeated supercells. Dangling-bond levels for silicon and germanium are calculated in Sec. III. The results are discussed in the context of the available experimental characterization. The conclusions are drawn in Sec. IV.

II. METHODS

The class of hybrid density functionals used in this paper are based on the generalized gradient approximation proposed by Perdew, Burke, and Ernzerhof (PBE)¹² and are obtained by replacing a fraction α of PBE exchange with Hartree-Fock exchange.¹³ The specific functional defined by the value $\alpha=0.25$ is supported by theoretical considerations and is known as PBE0.¹³ Our calculations are based on plane-wave basis sets and normconserving pseudopotentials.¹⁴ The pseudopotentials were generated at the PBE level and used in all calculations. For germanium, we included a nonlinear core correction to account for the overlap between valence and core states. The plane-wave basis sets were defined by an energy cutoff of 70 Ry. The defect calculations were performed with cubic supercells with a Brillouin-zone sampling restricted to the Γ point. For the determination of the band edges, primitive cells with a converged \mathbf{k} -point sampling were used. The integrable divergence of the Hartree-Fock exchange term is explicitly treated.¹⁵ Lattice parameters and structural relaxations were obtained at the PBE level.¹⁶⁻²⁰ For silicon, we calculated a

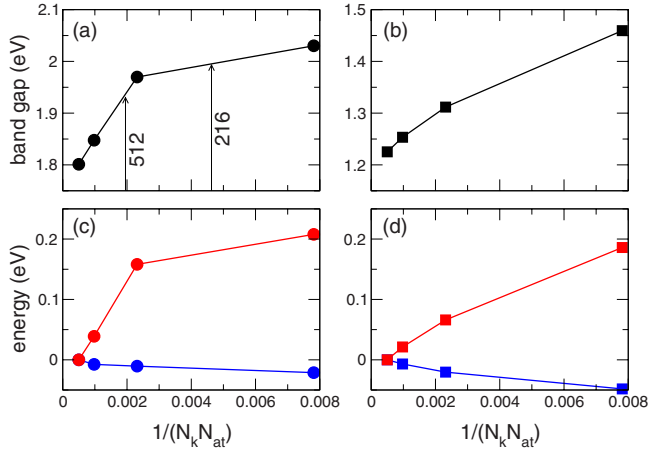


FIG. 1. (Color online) Convergence of band gaps and band edges for bulk Si [(a) and (c)] and Ge [(b) and (d)] with \mathbf{k} -point sampling. In (a), the \mathbf{k} -point samplings corresponding to a Γ -point sampling in 216- and 512-atom simulation cells are indicated. N_k being the number of \mathbf{k} points used and N_{at} the number of atoms in the simulation cell. In (c) and (d), blue/dark gray and red/gray labels correspond to the convergence error for the valence and conduction band, respectively.

lattice parameter of 5.48 Å and a bulk modulus of 88 GPa, which are in good agreement with the experimental values of 5.43 Å and 98 GPa, respectively. For germanium, the calculated lattice parameter (5.76 Å) and bulk modulus (62 GPa) similarly agree well with their experimental counterparts (5.66 Å and 75 GPa, respectively). Bulk and defect calculations were performed with the codes PWSCF²¹ and CPMD,²² respectively.

For the dangling bond, the relevant defect levels correspond to the charge-transition levels $\epsilon^{+/0}$ and $\epsilon^{0/-}$, which are obtained from the formation energies of the defect in its various charge states. The formation energy of a defect in its charge state q depends on the electron chemical potential μ and is given by²³

$$E_f^q(\mu) = E_{\text{tot}}^q - E_{\text{tot}}^0 + q(\epsilon_v + \mu + \Delta V) + E_{\text{corr}}, \quad (1)$$

where E_{tot}^q is the total energy of the defect in its charge state q , ϵ_v is the valence band for the defect-free bulk model, and ΔV is the change of the reference potential upon introduction of the defect. The total energies of the charged systems are corrected for the spurious interaction E_{corr} resulting from the periodic boundary conditions.²⁴ Charge transition levels correspond to values of the electron chemical potential for which two charge states of the defect have equal formation energies.

The dangling-bond defect was created by removing four neighboring atoms in a bulk supercell of 216 atoms. Nine of the ten dangling bonds generated in this way were then passivated by H atoms. The core structure of our model corresponds to that used in Ref. 7.

The choice of the model size resulted from the careful analysis of convergence issues related to the \mathbf{k} -point sampling and to the description of charged defects in periodically repeated supercells.²⁴ The first issue arises because the defect

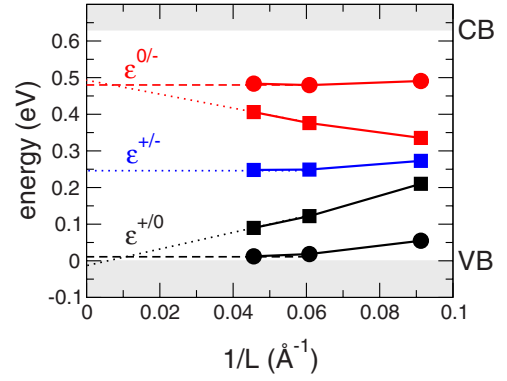


FIG. 2. (Color online) Convergence of charge-transition levels calculated for the Si dangling bond within PBE as a function of model size. The $\epsilon^{+/0}$ (black), $\epsilon^{0/-}$ (red/gray), and $\epsilon^{+/-}$ (blue/dark gray) transitions are either obtained directly from total-energy calculations (squares) or including corrections according to Ref. 24 (circles).

levels are calculated through a Brillouin-zone sampling restricted to the Γ point, for which the band edges have not yet reached convergence. Therefore, we considered the convergence of the band gaps and band edges as a function of \mathbf{k} -point sampling. Results for Si and Ge are given in Figs. 1(a) and 1(b), respectively. The results in Fig. 1 equivalently give the convergence as a function of cell size in case the \mathbf{k} -point sampling is restricted to the Γ point. For cell sizes as large as 512 atoms, band gaps are still overestimated by as much as ~ 0.1 eV. Thus, for typical supercell sizes used in the defect-level calculations, this overestimation needs to be accounted for. In Figs. 1(c) and 1(d), we show the convergence errors for the valence- and conduction-band edges of Si and Ge, respectively. For the 216-atom model, the Γ -point sampling leads to conduction-band errors of 0.18 and 0.12 eV and to valence-band errors of 0.02 and 0.03 eV for silicon and germanium, respectively. The defect levels reported in this paper are given with respect to the \mathbf{k} -point converged valence-band edge, which was determined using these corrections.

The second issue concerns the correction E_{corr} introduced above. We calculated the defect levels of the dangling bond in Si within PBE using models of different sizes, cf. Fig. 2. We estimated the correction E_{corr} using the dielectric constants determined experimentally (12 for Si and 16 for Ge). The effect of E_{corr} is appreciable for $\epsilon^{+/0}$ and $\epsilon^{0/-}$ as illustrated for the silicon dangling bond in Fig. 2. The levels calculated with and without E_{corr} extrapolate for infinite size to the same energy as expected. However, the errors at finite size are smaller when E_{corr} is included. In particular, the model based on the 64-atom cell is too small to achieve a reliable description even after accounting for E_{corr} . These considerations underlie our choice of adopting the model based on the 216-atom cell for the defect calculations. Indeed, for this model, E_{corr} amounts to 0.11 and 0.08 eV for Si and Ge, respectively, and its consideration reduces the error in the estimation of the charge-transition levels from ~ 0.1 to ~ 0.02 eV. Hence, these convergence tests show that, for the adopted model size, the interaction between the defect and its periodic images can be neglected provided the corrections E_{corr} are considered.

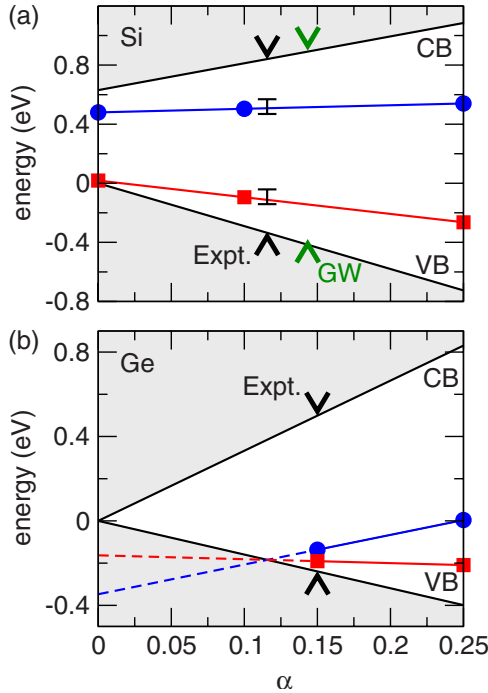


FIG. 3. (Color online) Valence-band edge (VB), conduction-band edge (CB), and dangling-bond defect levels vs fraction of Hartree-Fock exchange α for (a) Si and (b) Ge. Charge transition levels ϵ^{+0} (red/gray squares) and $\epsilon^{0/-}$ (blue/dark gray circles) are shown. Experimental band gaps are indicated. For Si, *GW* results for band-edge shifts (Ref. 11) and measured defect levels (Refs. 5 and 6) are reported in correspondence of the *GW* and the experimental band gaps, respectively.

III. RESULTS AND DISCUSSION

As well known, the PBE band gaps of silicon (0.63 eV) and germanium (0 eV) underestimate the experimental values (1.17 and 0.74 eV). At the PBE0 level, the calculated band gaps increase to 1.81 and 1.23 eV, respectively. While Hartree-Fock exchange systematically enhances the band gap,²⁵ the agreement with experiment is not impressively improved. This motivated us to consider the class of hybrid functionals obtained by varying the fraction α rather than focusing on one specific hybrid functional. The fraction α is equivalent to an effective static screening of Hartree-Fock exchange and its optimal value is naturally material dependent. For both silicon and germanium, the evolution of the valence- and conduction-band edges is found to be linear with α as shown in Fig. 3. For silicon, band-edge shifts obtained through *GW* calculations are included in correspondence of the *GW* band gap (1.3 eV)¹¹ showing good agreement with the shifts obtained with the hybrid functionals. While this result is encouraging, it is at present not clear to what extent it can be generalized to other materials. Therefore, we use the hybrid scheme with the free parameter α as a practical scheme to achieve insight into the experimental characterization. Correspondence with experimental band gaps of silicon and germanium is achieved for $\alpha=0.11$ and 0.15, respectively (Fig. 3).

We first focus on the dangling bond in silicon. Upon relaxation, the structure around the threefold coordinated sili-

TABLE I. Calculated charge-transition levels ϵ^{+0} and $\epsilon^{0/-}$ of the dangling bond referred to the valence-band edge in Si and Ge. Experimental values for Si are taken from Ref. 5. Values in parentheses correspond to linear extrapolations. Energies are in eV.

	α	E_g	ϵ^{+0}	$\epsilon^{0/-}$
Silicon				
PBE	0	0.63	0.02	0.48
PBE0	0.25	1.81	0.46	1.47
Intermediate	0.10	1.10	0.20	0.80
Experiment	–	1.17	0.26	0.84
Germanium				
PBE	0	0.00	(–0.17)	(–0.35)
PBE0	0.25	1.23	0.19	0.40
Intermediate	0.15	0.74	0.05	0.11
Experiment	–	0.74	–	–

con atom underwent minimal changes and preserved its axial symmetry. In the negative charge state, the back bonds are elongated by only 0.02 Å with respect to the equilibrium bond length. Contractions of 0.04 and 0.02 Å were found for the positive and neutral charge state, respectively. Charge transition levels ϵ^{+0} and $\epsilon^{0/-}$ were determined for PBE ($\alpha=0$), PBE0 ($\alpha=0.25$), and the intermediate case with $\alpha=0.10$. The defect levels evolve linearly with α as already observed for the band edges [Fig. 3(a)]. However, the defect levels shift only moderately when going from PBE to PBE0—in accord with a general trend observed for localized defect states.²⁰ In both the PBE and PBE0 schemes, the two charge-transition levels occur in the band gap (Table I). In particular, at $\alpha=0.10$ (for which the calculated band gap is close to the experimental value), the defect levels are found at 0.20 and 0.80 eV from the valence band, which are in excellent agreement with their experimental locations at 0.26 and 0.84 eV.⁵ In particular, the correlation energy is improved upon the PBE value (cf. Ref. 26).

Next, we applied the same scheme to the germanium dangling bond. The vanishing band gap of germanium within the PBE scheme undermines the reliability of structural relaxations. Therefore, to achieve model structures of the germanium dangling bond, we rescaled the relaxed 216-atom models of the silicon dangling bond in its various charge states by the ratio between the equilibrium lattice parameters of the two semiconductors.²⁷ We calculated charge-transition levels for PBE0 and for $\alpha=0.15$ (Table I). The evolution of the defect levels with α is illustrated in Fig. 3(b) where a linear dependence is assumed. In the PBE0 scheme, we found two charge-transition levels in the lower part of the band gap indicating the occurrence of three charge states in analogy with the dangling bond in silicon. However, the correlation energy of the dangling-bond defect in germanium is lower than in silicon—consistent with its more extended spin density (Fig. 4). In correspondence of the experimental band gap ($\alpha=0.15$), the charge-transition levels ϵ^{+0} and $\epsilon^{0/-}$ are found at 0.05 and 0.11 eV from the valence-band edge, respectively. In view of expectations for covalent semiconductors,⁸ it is reassuring that their location is in excellent agreement

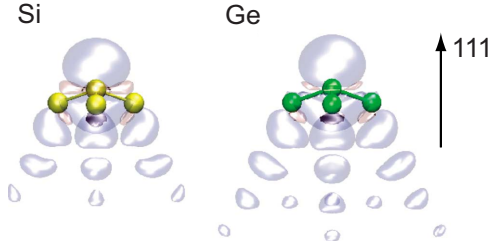


FIG. 4. (Color online) Isosurface of spin density for the dangling-bond defect in silicon and germanium. The dangling-bond axis is aligned along the $[111]$ direction. The atom carrying the dangling bond is shown with its three neighbors. The relative scale of the silicon and the germanium lattices is respected and the same isosurface is shown in both cases.

with the experimental charge neutrality level of germanium determined at 0.09 eV from the valence-band edge.^{9,10}

The defect levels of the dangling bond in germanium were recently addressed in Ref. 7 through semilocal functionals and G_0W_0 calculations. The defect levels obtained there with a semilocal functional are in qualitative agreement with the extrapolation of our defect levels to PBE—both showing inverted charge-transition levels (negative- U) below the valence-band edge (Table I). The G_0W_0 calculations support the defect-level location obtained with semilocal functionals. This picture is consistent with our results corresponding to a small fraction of Hartree-Fock exchange ($\alpha < 0.12$) but contrasts with the description achieved in correspondence of the experimental band gap ($\alpha = 0.15$). At present, it is difficult to adhere to one of these views solely on the basis of theoretical grounds. Therefore, it is important to examine the ensuing defect properties through comparison with experiment.

To address experimental observations,^{4,5} we used the calculated charge-transition levels in correspondence of the experimental band gaps. For both silicon and germanium, we empirically introduced a Gaussian broadening of 0.1 eV corresponding to the measured density of dangling-bond states at Si-SiO₂ interfaces.⁶ We relied on a statistical description which accounts for possible negative- U behavior introduced by the broadening.

First, we address the density of dangling-bond states in view of interpreting capacitance-voltage experiments.^{4,5} For silicon, the characteristic double-peak structure in the density of dangling-bond states is reproduced [Fig. 5(a)]. Applied to germanium, the small separation between the $\epsilon^{+/0}$ and $\epsilon^{0/-}$ charge-transition levels leads to a single peak just above the valence-band maximum [Fig. 5(b)]. Thus, the density of dangling-bond states in germanium occurs in a region of the band gap where the valence-band tails still give a sizeable contribution to the defect density. Additional broadening effects are expected ensuing from the degeneracy between the defect levels and the continuum of band tails, which is not properly described in our models. These considerations provide an explanation for the absence of a distinct signature in the experimental defect density.⁴

Our results also provide a rationale for the different ESR activities of the dangling-bond defects at Si-SiO₂ and Ge-GeO₂ interfaces. The large separation between the $\epsilon^{+/0}$

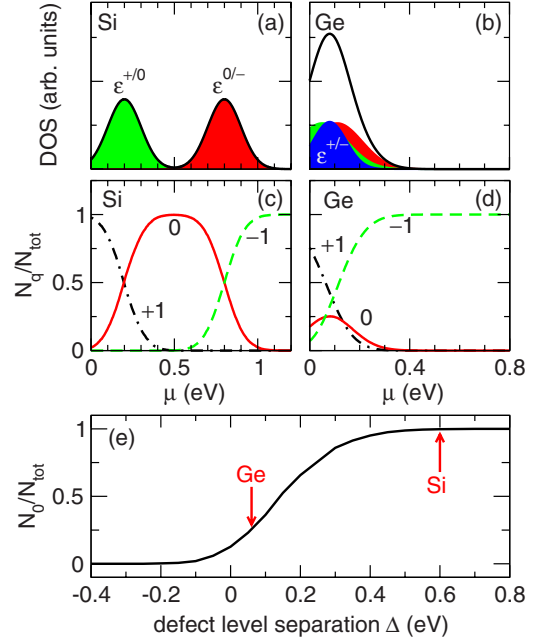


FIG. 5. (Color online) Densities of dangling-bond states (DOS) in (a) Si and (b) Ge and their decomposition into charge-transition levels for electron chemical potential μ sweeping through the respective band gaps. The corresponding occupation of the three charge states is shown in (c) and (d). In (e), the fraction of ESR-active dangling bonds in correspondence of charge neutrality is given vs defect-level separation $\Delta = \epsilon^{0/-} - \epsilon^{+/0}$. The separation calculated in this paper for Si and Ge are indicated by arrows. We used a standard deviation of 0.1 eV for the distribution of charge-transition levels (Ref. 6).

and $\epsilon^{0/-}$ levels of the silicon dangling bond ensures a high fraction of ESR-active neutral dangling bonds at charge neutrality [Figs. 5(c) and 5(e)]. Conversely, the quasi-negative- U character of the dangling-bond levels in germanium significantly suppresses the amount of neutral dangling bonds [Figs. 5(d) and 5(e)]. For the values adopted in our model, we derived for germanium a reduction by a factor of 4 as compared to silicon. However, larger level broadenings or a smaller charge-transition level separation $\Delta = \epsilon^{0/-} - \epsilon^{+/0}$ could easily further suppress the ESR activity.

IV. CONCLUSIONS

We determined the energy levels of the dangling-bond defect in silicon and germanium through the use of hybrid density functionals. For the silicon dangling bond, the charge-transition levels $\epsilon^{+/0}$ and $\epsilon^{0/-}$ were found at $\epsilon_v + 0.2$ eV and $\epsilon_v + 0.8$ eV, respectively, which are in very good agreement with experiment. For the germanium dangling bond, our calculations yield two very close charge-transition levels in the band gap at only ~ 0.1 eV from the valence-band edge. This location is consistent with the charge neutrality level determined experimentally.^{9,10} Furthermore, the proximity to the valence band and the small correlation energy provide a plausible explanation for the absence of clear defect signatures in electrical and ESR experiments.⁴

In view of the present results, it is interesting to comment on the Fermi-level pinning at Si-metal and Ge-metal interfaces. The pinning at such interfaces is generally ascribed to metal-induced gap states and is therefore expected to be largely independent of the metal.⁸ However, recent experiments in which the metal is varied show that the pinning level ranges between 0.26 and 0.70 eV from the valence-band edge for silicon and between 0.04 and 0.18 eV for germanium.¹⁰ These values closely correspond to the charge-transition levels calculated in this paper suggesting that the

dangling-bond states contribute to the confinement of the pinning levels at Si-metal and Ge-metal interfaces.

ACKNOWLEDGMENTS

The support from the Swiss National Science Foundation (Grants No. 200020-111747 and No. 200020-119733) is acknowledged. The calculations were performed on the BlueGene of EPFL and at CSCS.

-
- ¹C. O. Chui, S. Ramanathan, B. B. Triplett, P. McIntyre, and K. C. Saraswat, *IEEE Electron Device Lett.* **23**, 473 (2002).
²H. Shang, H. Okorn-Schmidt, J. Ott, P. Kozlowski, S. Steen, E. C. Jones, H. S. Wong, and W. Hanesch, *IEEE Electron Device Lett.* **24**, 242 (2003).
³V. V. Afanas'ev and A. Stesmans, *Appl. Phys. Lett.* **84**, 2319 (2004).
⁴V. V. Afanas'ev, Y. G. Fedorenko, and A. Stesmans, *Appl. Phys. Lett.* **87**, 032107 (2005).
⁵E. H. Poindexter, G. J. Gerardi, M.-E. Rueckel, P. J. Caplan, N. M. Johnson, and D. K. Biegelsen, *J. Appl. Phys.* **56**, 2844 (1984).
⁶M. J. Uren, J. H. Stathis, and E. Cartier, *J. Appl. Phys.* **80**, 3915 (1996).
⁷J. R. Weber, A. Janotti, P. Rinke, and C. G. Van de Walle, *Appl. Phys. Lett.* **91**, 142101 (2007).
⁸J. Tersoff, *Phys. Rev. Lett.* **52**, 465 (1984).
⁹A. Dimoulas, P. Tsipas, A. Sotiropoulos, and E. K. Evangelou, *Appl. Phys. Lett.* **89**, 252110 (2006).
¹⁰T. Nishimura, K. Kita, and A. Toriumi, *Appl. Phys. Lett.* **91**, 123123 (2007).
¹¹R. Shaltaf, G.-M. Rignanese, X. Gonze, F. Giustino, and A. Pasquarello, *Phys. Rev. Lett.* **100**, 186401 (2008).
¹²J. P. Perdew, K. Burke, and M. Ernzerhof, *Phys. Rev. Lett.* **77**, 3865 (1996).
¹³J. P. Perdew, M. Ernzerhof, and K. Burke, *J. Chem. Phys.* **105**, 9982 (1996).
¹⁴N. Troullier and J. L. Martins, *Phys. Rev. B* **43**, 1993 (1991).
¹⁵F. Gygi and A. Baldereschi, *Phys. Rev. B* **34**, 4405 (1986).
¹⁶P. Broqvist and A. Pasquarello, *Appl. Phys. Lett.* **89**, 262904 (2006).
¹⁷P. Broqvist and A. Pasquarello, *Appl. Phys. Lett.* **90**, 082907 (2007).
¹⁸F. Devynck, F. Giustino, P. Broqvist, and A. Pasquarello, *Phys. Rev. B* **76**, 075351 (2007).
¹⁹P. Broqvist, A. Alkauskas, and A. Pasquarello, *Appl. Phys. Lett.* **92**, 132911 (2008).
²⁰A. Alkauskas, P. Broqvist, and A. Pasquarello, *Phys. Rev. Lett.* **101**, 046405 (2008).
²¹We used the pwscf code provided at <http://www.quantum-espresso.org/>
²²R. Car and M. Parrinello, *Phys. Rev. Lett.* **55**, 2471 (1985); CPMD, Copyright IBM Corp 1990–2006, Copyright MPI für Festkörperforschung Stuttgart 1997–2001; J. Hutter and A. Curioni, *ChemPhysChem* **6**, 1788 (2005).
²³C. G. Van de Walle and J. Neugebauer, *J. Appl. Phys.* **95**, 3851 (2004).
²⁴G. Makov and M. C. Payne, *Phys. Rev. B* **51**, 4014 (1995).
²⁵J. Paier, M. Marsman, K. Hummer, G. Kresse, I. C. Gerber, and J. G. Ángyán, *J. Chem. Phys.* **124**, 154709 (2006).
²⁶J. E. Northrup, *Phys. Rev. B* **40**, 5875 (1989).
²⁷To support this procedure, we carried out full structural relaxations within PBE0 for a 64-atom supercell finding defect levels differing by at most 0.05 eV.